

# Molecular Structure of 1-(Difluoroboryl)pentaborane(9), 1-(F<sub>2</sub>B)B<sub>5</sub>H<sub>8</sub>, in the Gas Phase As Determined by Electron Diffraction and Supported by *ab Initio* and IGLO Calculations

Paul T. Brain, David W. H. Rankin,\* Heather E. Robertson, and Ian L. Alberts

Department of Chemistry, University of Edinburgh, West Mains Road, Edinburgh, EH9 3JJ, U.K.

Matthias Hofmann and Paul von Ragué Schleyer

Institut für Organische Chemie der Universität Erlangen-Nürnberg, Henkestrasse 24, D-91054 Erlangen, Germany

Received August 18, 1993\*

The structure of gaseous 1-(difluoroboryl)pentaborane(9), 1-(F<sub>2</sub>B)B<sub>5</sub>H<sub>8</sub>, has been determined by electron diffraction. The results confirm that the molecule consists of a pentaborane(9) cage substituted at the apical boron atom, B(1), by a difluoroboryl group; the BF<sub>2</sub> moiety is free to rotate about the *exo* B–B bond. Salient structural parameters (*r*<sub>a</sub>) are *r*(B–B)(base–base) = 181.2(6), *r*(B–B)(base–apex) = 170.6(4), *r*(B–B)(apex–*exo*) = 167.6(7), *r*(B–F) = 132.2(3), *r*(B–H<sub>a</sub>) = 119.5(13), and *r*(B–H<sub>b</sub>) = 138.9(11) pm; FBF = 115.4(6)°, B–H<sub>a</sub> “rise” (above basal plane) = 1.9(33)°, and B–H<sub>b</sub> “dip” (below basal plane) = 67.7(29)°. These conclusions are supported by *ab initio* (MP2/6-31G\* or DZP level) optimizations of the molecular geometry and by comparison of the calculated <sup>11</sup>B NMR chemical shifts [IGLO(DZ)//GED level] with the experimental NMR data.

## Introduction

Although increasing numbers of compounds containing *exo* 2c–2e B–B bonds to boron hydrides have been described recently, their characterization has relied mainly on modern spectroscopic techniques and chemical analysis.<sup>1–5</sup> Few structural studies have been published, and those that are available have been confined to X-ray diffraction of single crystals.<sup>6–14</sup> No structural determinations have been carried out on gaseous molecules. Of the many pentaborane(9) derivatives that have been synthesized, moreover, only pentaborane(9),<sup>15</sup> 1- and 2-methylpentaborane(9)<sup>16</sup> and 1- and 2-silylpentaborane(9)<sup>16</sup> have been studied in the gas phase by electron diffraction (GED).

Since the 1-(dihaloboryl)pentaborane(9) derivatives, 1-(X<sub>2</sub>B)-B<sub>5</sub>H<sub>8</sub> (X = F, Cl, or Br), are volatile and thermally stable enough

to be studied in the gas phase,<sup>17–19</sup> it was decided, as part of a wider investigation of compounds containing B–B bonds,<sup>19–21</sup> to initiate a study of these compounds in terms of their electron-diffraction patterns. Not only is such a study important to an understanding of the structural and electronic properties of this homologous series of molecules, but it also serves to increase the database in an otherwise sparsely documented area of boron hydride chemistry. The first results, based on an electron-diffraction study of gaseous 1-(difluoroboryl)pentaborane(9), are presented here.

It has recently become possible to predict the structures of relatively large boranes using the combined *ab initio*/IGLO/NMR method.<sup>22–24</sup> In this approach, various structures derived from experiment and from *ab initio* geometry optimizations are assessed by means of IGLO (individual gauge for localized orbitals)<sup>25</sup> NMR calculations. The <sup>11</sup>B chemical shifts obtained by this method for various geometries are compared with the experimental chemical shifts. Using geometries optimized at electron-correlated levels of theory (*e.g.* MP2(fc)/6-31G\*, *i.e.* with a basis set including polarization functions), the agreement between experimental and IGLO <sup>11</sup>B chemical shifts has been found to be consistently good.<sup>24a</sup>

- \* Author to whom correspondence should be addressed.  
 • Abstract published in *Advance ACS Abstracts*, April 15, 1994.
- (1) Gaines, D. F.; Iorns, T. V.; Clevenger, E. N. *Inorg. Chem.* **1971**, *10*, 1096.
  - (2) Steck, S. J.; Pressley, G. A., Jr.; Stafford, F. E.; Dobson, J.; Schaeffer, R. *Inorg. Chem.* **1969**, *8*, 830.
  - (3) Dobson, J.; Gaines, D.; Schaeffer, R. *J. Am. Chem. Soc.* **1965**, *87*, 4072.
  - (4) Hawthorne, M. F.; Pilling, R. L.; Stokely, P. F. *J. Am. Chem. Soc.* **1965**, *87*, 1893.
  - (5) Corcoran, E. W., Jr.; Sneddon, L. G. *J. Am. Chem. Soc.* **1984**, *106*, 7793, and references therein.
  - (6) Boocock, S. K.; Greenwood, N. N.; Kennedy, J. D.; McDonald, W. S.; Staves, J. *J. Chem. Soc., Dalton Trans.* **1980**, 790.
  - (7) Brown, G. M.; Pinson, J. W.; Ingram, L. L., Jr. *Inorg. Chem.* **1979**, *18*, 1951.
  - (8) Barrett, S. A.; Greenwood, N. N.; Kennedy, J. D.; Thornton-Pett, M. *Polyhedron* **1985**, *4*, 1981.
  - (9) Grimes, R.; Wang, F. E.; Lewin, R.; Lipscomb, W. N. *Proc. Natl. Acad. Sci. U.S.A.* **1961**, *47*, 996.
  - (10) Pretzer, W. R.; Rudolph, R. W. *J. Chem. Soc., Chem. Commun.* **1974**, 629.
  - (11) Šubrtová, V.; Líněk, A.; Hašek, J. *Acta Crystallogr., Sect. B: Struct. Crystallogr. Cryst. Chem.* **1982**, *38*, 3147.
  - (12) Micciche, R. P.; Plotkin, J. S.; Sneddon, L. G. *Inorg. Chem.* **1983**, *22*, 1765.
  - (13) Boocock, S. K.; Greenwood, N. N.; Kennedy, J. D.; McDonald, W. S.; Staves, J. *J. Chem. Soc., Dalton Trans.* **1981**, 2573.
  - (14) Briguglio, J. J.; Carroll, P. J.; Corcoran, E. W., Jr.; Sneddon, L. G. *Inorg. Chem.* **1986**, *25*, 4618.
  - (15) Greatrex, R.; Greenwood, N. N.; Rankin, D. W. H.; Robertson, H. E. *Polyhedron* **1987**, *6*, 1849.
  - (16) Wieser, J. D.; Moody, D. C.; Huffman, J. C.; Hilderbrandt, R. L.; Schaeffer, R. *J. Am. Chem. Soc.* **1975**, *97*, 1074.

- (17) Gaines, D. F.; Heppert, J. A.; Coons, D. E.; Jorgenson, M. W. *Inorg. Chem.* **1982**, *21*, 3662.
- (18) Saulys, D. A.; Morrison, J. A. *Inorg. Chem.* **1990**, *29*, 4174.
- (19) Brain, P. T. D. Phil. Thesis, Oxford University, 1991.
- (20) Brain, P. T.; Downs, A. J.; Fanfarillo, M.; Goode, M. J.; Massey, A. G.; Rankin, D. W. H.; Robertson, H. E. *J. Mol. Struct.* **1989**, *192*, 163.
- (21) Brain, P. T.; Downs, A. J.; Maccallum, P.; Rankin, D. W. H.; Robertson, H. E.; Forsyth, G. A. *J. Chem. Soc., Dalton Trans.* **1991**, 1195.
- (22) Schleyer, P. v. R.; Bühl, M.; Fleischer, U.; Koch, W. *Inorg. Chem.* **1990**, *29*, 153.
- (23) Bühl, M.; Schleyer, P. v. R. *Angew. Chem., Inter. Ed. Engl.* **1990**, *29*, 886.
- (24) For other examples, see: (a) Bühl, M.; Schleyer, P. v. R. *J. Am. Chem. Soc.* **1992**, *114*, 477. (b) Hnyk, D.; Vajda, E.; Bühl, M.; Schleyer, P. v. R. *Inorg. Chem.* **1992**, *31*, 2464. (c) Mebel, A. M.; Charkin, O. P.; Bühl, M.; Schleyer, P. v. R. *Inorg. Chem.* **1993**, *32*, 463. (d) Onak, T.; Tseng, J.; Diaz, M.; Tran, D.; Arias, J.; Herrera, S.; Brown, D. *Inorg. Chem.* **1993**, *32*, 487.
- (25) (a) Kutzelnigg, W. *Isr. J. Chem.* **1980**, *19*, 193. (b) Schindler, M.; Kutzelnigg, W. *J. Chem. Phys.* **1982**, *76*, 1919. (c) Review: Kutzelnigg, W.; Fleischer, U.; Schindler, M. in *NMR, Basic Principles and Progress*; Springer Verlag: Berlin, 1990; Vol. 23, p 165.

**Table 1.** Nozzle-to-Plate Distances, Weighting Functions, Correlation Parameters, Scale Factors, and Electron Wavelengths

molecule	nozzle-to-plate dist/mm	$\Delta s/\text{nm}^{-1}$	$s_{\text{min}}/\text{nm}^{-1}$	$sw_1/\text{nm}^{-1}$	$sw_2/\text{nm}^{-1}$	$s_{\text{max}}/\text{nm}^{-1}$	correln param $p/h$	scale factor, $k^a$	electron wavelength <sup>b</sup> /pm
1-(F <sub>2</sub> B)B <sub>5</sub> H <sub>8</sub>	262.5	2	20	40	138	162	0.4417	0.763(16)	5.686
	203.5	4	40	60	172	204	-0.0899	0.679(15)	5.687

<sup>a</sup> Figures in parentheses are the estimated standard deviations. <sup>b</sup> Determined by reference to the scattering pattern of benzene vapor.

In the electron-diffraction analysis, the parameters defining the structures of boranes, especially those for the boron framework, are subject to significant correlation.<sup>26</sup> Moreover, it is possible that several geometries will fit the electron-scattering data more or less equally well, and additional information (e.g. spectroscopic or theoretical) is required to decide which of the options is correct.<sup>27</sup> The electron-scattering pattern of 1-(F<sub>2</sub>B)B<sub>5</sub>H<sub>8</sub> has been analyzed, and the refined structure is found to be in good agreement with the geometry proposed by the *ab initio* study. The accuracy of the structure is further substantiated by *ab initio* energy and <sup>11</sup>B chemical shift calculations.

### Experimental Section

**Synthesis.** 1-(Difluoroboryl)pentaborane(9) was prepared by the reaction of bis(trifluoromethyl)mercury, Hg(CF<sub>3</sub>)<sub>2</sub>, with 1-(dichloroboryl)pentaborane(9) using a method similar to that reported recently by Morrison and Saulys.<sup>18,19</sup> The purity of the compound was checked by reference (i) to the IR spectrum of the vapor and/or that of a solid film at 77 K,<sup>19</sup> (ii) to the <sup>1</sup>H, <sup>19</sup>F and <sup>11</sup>B NMR spectra of a [<sup>2</sup>H<sub>8</sub>] toluene solution,<sup>18,19</sup> and (iii) to the mass spectrum of the vapor.<sup>18,19</sup>

**Electron-Diffraction Measurements.** Electron-scattering measurements were recorded on Kodak Electron Image plates using the Edinburgh gas-diffraction apparatus operating at ca. 44.5 kV (electron wavelength ca. 5.7 pm).<sup>28</sup> Nozzle-to-plate distances were ca. 204 and 263 mm yielding data in the  $s$  range 20–204 nm<sup>-1</sup>; two usable plates were obtained at each distance.

Because of the sensitivity of the compound to hydrolysis, the use of the normal stainless-steel nozzle was considered to be undesirable. Instead, an all-glass inlet nozzle, designed originally for the diffraction of gallane,<sup>29</sup> was employed. This permitted the passage of the vapor into the diffraction chamber with exposure limited to Pyrex glass surfaces. The sample and nozzle were held at ca. 291 K during the exposure periods; prior to the first exposure at each camera distance, a small amount of the sample was pumped into the diffraction chamber to condition all the surfaces exposed to the vapor.

The scattering patterns of benzene were also recorded for the purpose of calibration; these were analyzed in exactly the same way as those of the pentaborane(9) derivative so as to minimize systematic errors in the wavelengths and camera distances. Nozzle-to-plate distances, weighting functions used to set up the off-diagonal weight matrix, correlation parameters, final scale factors, and electron wavelengths for the measurements are collected together in Table 1.

The electron-scattering patterns were converted into digital form using a computer-controlled Joyce-Loebl MDM6 microdensitometer with a scanning program described elsewhere.<sup>30</sup> The programs used for data reduction<sup>30</sup> and least-squares refinement<sup>31</sup> have been described previously; the complex scattering factors employed were those listed by Fink and Ross.<sup>32</sup>

- (26) Brain, P. T.; Hnyk, D.; Rankin, D. W. H.; Bühl, M.; Schleyer, P. v. R. *Polyhedron*, in press.
- (27) For example, see: (a) Hargittai, I., Hargittai, M., Eds.; *Stereochemical Applications of Gas-Phase Electron Diffraction, Part A*; VCH: Weinheim, Germany, 1990; p 301. (b) Hnyk, D.; Bühl, M.; Schleyer, P. v. R.; Volden, H. V.; Gundersen, S.; Müller, J.; Paetzold, P. *Inorg. Chem.* **1993**, *32*, 2442.
- (28) Huntley, C. M.; Laurensen, G. S.; Rankin, D. W. H. *J. Chem. Soc., Dalton Trans.* **1980**, 954.
- (29) Pulham, C. R.; Downs, A. J.; Goode, M. J.; Rankin, D. W. H.; Robertson, H. E. *J. Am. Chem. Soc.* **1991**, *113*, 5149.
- (30) Cradock, S.; Koproński, J.; Rankin, D. W. H. *J. Mol. Struct.* **1981**, *77*, 113.
- (31) Boyd, A. S. F.; Laurensen, G. S.; Rankin, D. W. H. *J. Mol. Struct.* **1981**, *71*, 217.
- (32) Ross, A. W.; Fink, M.; Hilderbrandt, R. *International Tables for Crystallography*; Wilson, A. J. C., Ed.; Kluwer Academic Publishers: Dordrecht, The Netherlands, Boston, MA, and London, 1992; Vol. C, p 245.

**Table 2.** Structural Parameters for 1-(F<sub>2</sub>B)B<sub>5</sub>H<sub>8</sub> (Distances in pm, Angles in deg)

param <sup>a</sup>		electron diffraction <sup>b</sup> ( $r_a$ )	theoretical <sup>c</sup> ( $r_e$ )
$p_1$	$r(\text{B-B})$ (base-base)	181.2(6)	179.3/178.0
$p_2$	$r(\text{B-B})$ (base-apex)	170.6(4)	169.0
$p_3$	$r(\text{B-B})$ (apex-exo)	167.6(7)	167.1
$p_4$	$r(\text{B-F})$	132.2(3)	134.0
$p_5$	$r(\text{B-H})$ (terminal)	119.5(13)	118.6
$p_6$	$r(\text{B-H})$ (bridge)	138.9(11)	134.3
$p_7$	FBF	115.4(6)	114.9
$p_8$	B-H <sub>1</sub> "rise" (above basal plane)	1.9(33)	7.2
$p_9$	B-H <sub>6</sub> "dip" (below basal plane)	67.7(29)	63.6/62.9
$p_{10}$	barrier to BF <sub>2</sub> rotation, $V_0$	0.0(fixed)	0.08 <sup>d</sup>

<sup>a</sup> For definitions of parameters, see the text. Figures in parentheses are the estimated standard deviations. <sup>b</sup> Electron diffraction of the vapor assuming free rotation of the BF<sub>2</sub> group. <sup>c</sup> Optimized geometry at the MP2(fc)/6-31G\* level based on a 0° BF<sub>2</sub> twist (F atoms lying above H<sub>6</sub>). <sup>d</sup>  $V_0 = E(\text{geometry with BF}_2 \text{ twist angle} = 45^\circ) - E(\text{geometry with BF}_2 \text{ twist angle} = 0^\circ)$ . Calculated at the MP2(fc)/6-31G\* level.

**Theoretical Calculations.** *Ab initio* computations employed standard procedures and basis sets<sup>33–38</sup> using the Gaussian92 (Erlangen)<sup>39</sup> and CADPAC5 (Edinburgh)<sup>40</sup> programs. <sup>11</sup>B NMR chemical shifts have been calculated using the IGLO method<sup>25</sup> employing a Huzinaga basis set<sup>41</sup> of double- $\zeta$  (DZ) quality.<sup>25c</sup> The theoretical chemical shifts (Table 6) have been referenced to BF<sub>3</sub>·OEt<sub>2</sub>, as described elsewhere,<sup>24a</sup> and are given in the notation "level of the chemical shift calculation//geometry employed". The calculations were performed on the Convex C3840 and Cray facilities at the Rutherford-Appleton Laboratory and the University of London Computing Centre, the Convex C220 of the Institut für Organische Chemie der Universität Erlangen-Nürnberg, and on a Cray YMP-8 of the Leibniz Rechenzentrum in Munich.

### Molecular Model

On the basis of the spectroscopic evidence,<sup>17–19</sup> the molecular model used to generate the atomic coordinates of 1-(F<sub>2</sub>B)B<sub>5</sub>H<sub>8</sub> was based on the structure established for B<sub>5</sub>H<sub>9</sub><sup>15</sup> except, of course, that the terminal hydrogen attached to the apical boron atom, B(1), was replaced by a BF<sub>2</sub> unit. In the final refinements, such a model was described by the parameters listed in Table 2; the atom numbering scheme is shown in Figure 3.

**The Boron Cage.** The B<sub>5</sub>H<sub>8</sub> cage was assumed to possess C<sub>4v</sub> symmetry with one terminal hydrogen atom (H<sub>1</sub>) associated with each boron atom and with four bridging hydrogen atoms (H<sub>6</sub>),

- (33) See: Hehre, W.; Radom, L.; Schleyer, P. v. R.; Pople, J. A. *Ab Initio Molecular Orbital Theory*; Wiley: New York, 1986.
- (34) Huzinaga, S. *J. Chem. Phys.* **1965**, *42*, 1293.
- (35) Dunning, T. H. *J. Chem. Phys.* **1970**, *53*, 2823.
- (36) Dunning, T. H.; Hay, P. J. *Modern Theoretical Chemistry*; Schaefer, H. F., Ed.; Plenum: New York, 1977; Vol. 3, p 1.
- (37) McLean, A. D.; Chandler, G. S. *J. Chem. Phys.* **1980**, *72*, 5639.
- (38) Dunning, T. H. *J. Chem. Phys.* **1971**, *55*, 716.
- (39) Frisch, M. J.; Trucks, G. W.; Head-Gordon, M.; Gill, P. M. W.; Wong, M. W.; Foresman, J. B.; Schlegel, H. B.; Raghavachari, K.; Robb, M. A.; Replogle, E. S.; Gomperts, R.; Andres, J. L.; Binkley, J. S.; Gonzalez, C.; Martin, R.; Fox, D. J.; DeFrees, D. J.; Baker, J.; Stewart, J. J. P.; Pople, J. A. Gaussian Inc., Pittsburgh, PA, 1992.
- (40) CADPAC5: The Cambridge Analytical Derivatives Package, Issue 5, Cambridge, U.K., 1992. A suite of quantum-chemistry programs developed by R. D. Amos with contributions from I. L. Alberts, J. S. Andrews, S. M. Colwell, N. C. Handy, D. Jayatilaka, P. J. Knowles, R. Kobayashi, N. Koga, K. E. Laidig, P. E. Maslen, C. W. Murray, J. E. Rice, J. Sanz, E. D. Simandiras, A. J. Stone, and M.-D. Su.
- (41) Huzinaga, S. *Approximate Atomic Wavefunctions*; University of Alberta: Edmonton, Canada, 1971.

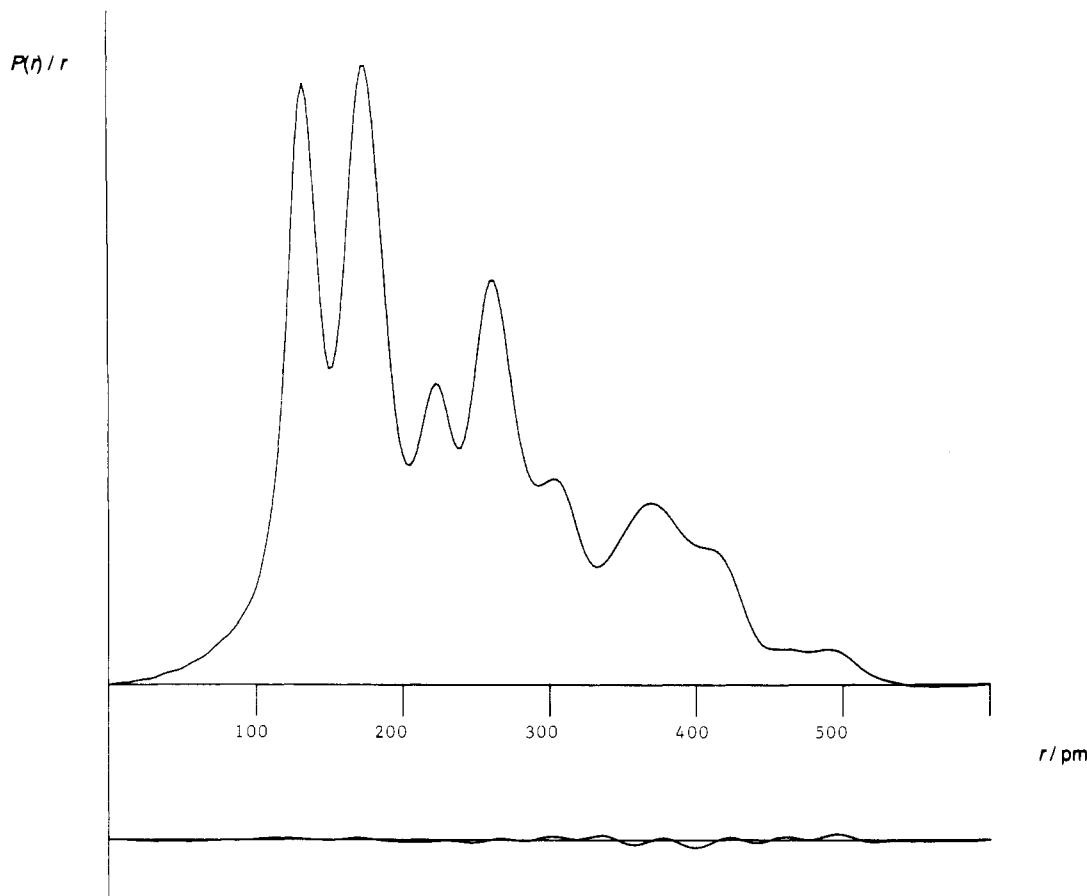


**Figure 1.** Observed and final weighted radial-distribution curves for 1-(F<sub>2</sub>B)B<sub>5</sub>H<sub>8</sub>. Before Fourier inversion the data were multiplied by  $s \cdot \exp[-(0.00002s^2)/(Z_B - f_B)(Z_F - f_F)]$ .

each one equidistant from two boron atoms. The cage structure was then defined by two different B–B interatomic distances (base–base and base–apex), two B–H interatomic distances (terminal and bridging), and two angles defining the orientation of the B–H<sub>i</sub> and B–H<sub>b</sub>–B units. These angles were chosen to be measured relative to the basal plane of the B<sub>5</sub> pyramid, upward (toward the apex) for the B–H<sub>i</sub> unit (“H<sub>i</sub> rise”) and downward (away from the apex) for the B–H<sub>b</sub>–B unit (“H<sub>b</sub> dip”).

**The Fluoroboryl Group.** The B–BF<sub>2</sub> moiety, with local C<sub>2v</sub> symmetry (C<sub>2</sub> axis coincident with the C<sub>4</sub> axis of the boron cage), was defined by four parameters: the B–B (apex–exo) and the B–F distances, the FBF angle, and a parameter defining the location of the fluorine atoms relative to the basal boron and the hydrogen atoms. In the initial refinements this parameter was defined as a torsion angle allowing the BF<sub>2</sub> group to twist about the B–B (apex–exo) bond, such that the plane of the BF<sub>2</sub> unit did not necessarily contain two of the bridging hydrogen atoms (torsion angle = 0°) but could take up an orientation between the two different types of hydrogen atom when viewed along the B–B (exo–apex) axis (see Figure 3b). In the later refinements, however, this parameter was defined as a potential energy barrier to free rotation (V<sub>0</sub>) of the BF<sub>2</sub> moiety about the B–B (apex–exo) bond. This was achieved by representing the rotation as a set of four fixed conformations of the BF<sub>2</sub> group over the range 0° ≤ φ ≤ 45° of the rotation angle, φ (φ = 0° defined as having two bridging hydrogens in the BF<sub>2</sub> plane). Thus, the continuous torsion-sensitive distance distribution was approximated by calculating the nonbonding distances r(F⋯B) and r(F⋯H) at angle increments Δφ = 11.25°; 48 distinct torsion-sensitive distances were generated by this scheme. The low-barrier classical approximation for the probability distribution of the rotation angle (φ) was adopted

$$P(\phi) = N[\exp(-V(\phi)/RT)]$$

and the potential function was assumed to be of the form

$$V(\phi) = V_0[1 - \cos(4\phi)]$$

The relative multiplicity of each of the 16 r(F⋯B) and the 32 r(F⋯H) distinct nonbonded distances was weighted according to P(φ).

The overall structure, with C<sub>2v</sub> symmetry for a 0° rotation of the BF<sub>2</sub> group, was then defined by 10 independent parameters.

## Results

**Refinement of the Structure.** The radial-distribution curve for 1-(F<sub>2</sub>B)B<sub>5</sub>H<sub>8</sub> (Figure 1) shows five peaks at distances shorter than 330 pm; these occur near 133, 173, 223, 252, and 302 pm. The peaks at r < 200 pm correspond to scattering from bonded atom pairs; the B–H (bridging and terminal) and B–F distances contribute to the peak at ca. 133 pm, whereas the peak at ca. 173 pm has contributions from the three different B–B bonded distances. The F⋯F nonbonded pair contributes mainly to the peak at ca. 223 pm (together with some H⋯H nonbonded distances) and the B⋯H nonbonded pairs are identified with the peak at ca. 252 pm, augmented by contributions from the B(apex)⋯F and B⋯B (base⋯base) nonbonded pairs; the feature at ca. 302 pm is attributed to the B⋯B (base⋯exo) nonbonded pairs. The radial-distribution curve at r > 330 pm consists of several broad features encompassing the B(base)⋯F and H⋯F nonbonded distances in the molecule.

Initial refinements of the molecular structure employing a static model, *i.e.* incorporating p<sub>10</sub> as a BF<sub>2</sub> “twist angle”, yielded parameters similar to those reported in Table 2, with p<sub>10</sub> = 14.5(36)°. However, the low potential energy barrier to rotation calculated *ab initio* (ca. 0.25 kJ mol<sup>-1</sup> at the MP2/TZ2P level, see below) together with the refined large amplitudes of vibration

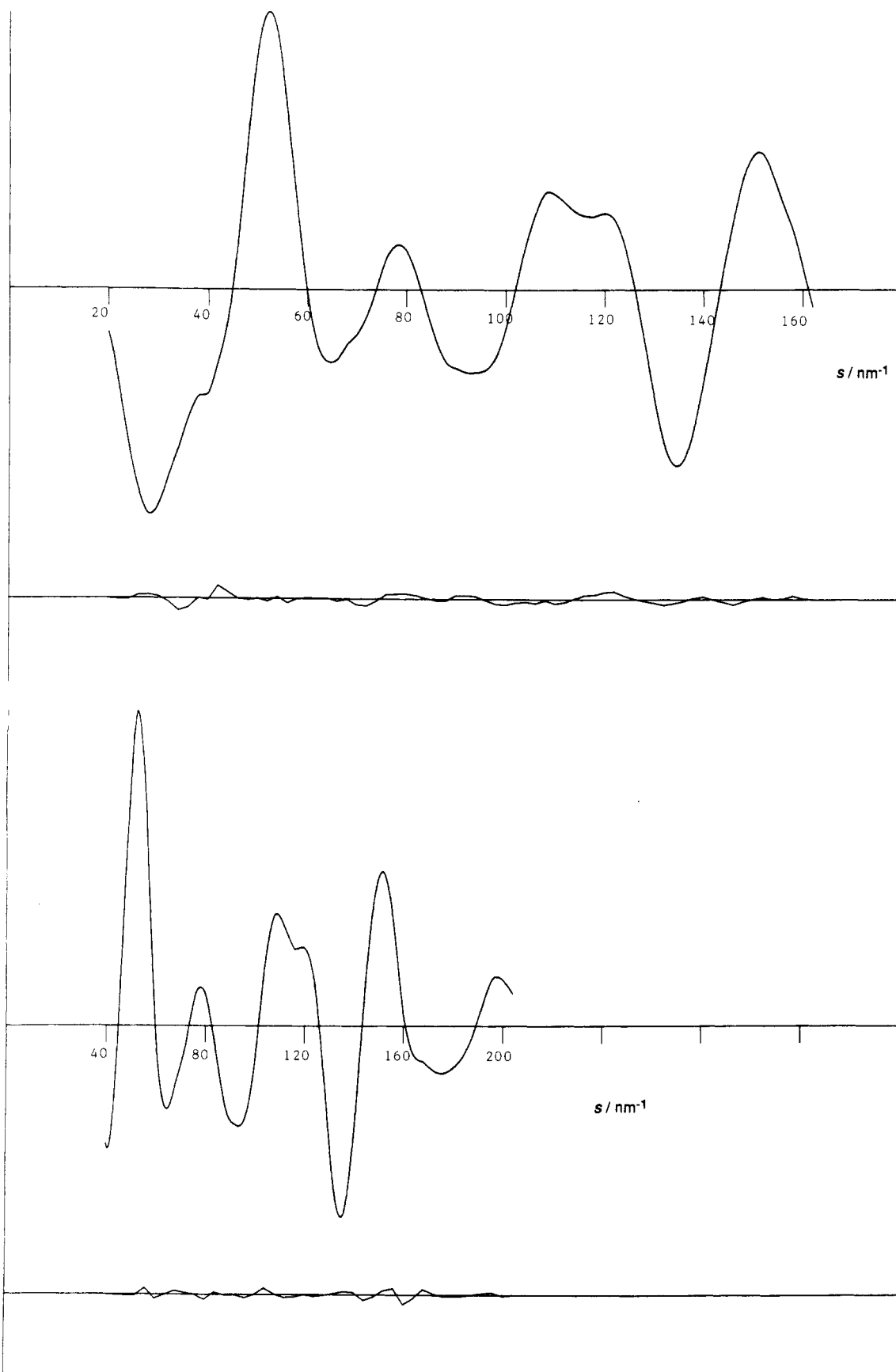


**Figure 2.** Observed and final weighted difference molecular-scattering intensity curves for 1-(F<sub>2</sub>B)B<sub>5</sub>H<sub>8</sub>. Nozzle-to-plate distances were (a, top) 262.5 and (b, bottom) 203.5 mm.

for the B(base)⋯F nonbonded pairs, *ca.* 16(1) pm, were indicative of a structure in which the barrier to rotation of the BF<sub>2</sub> moiety about the B–B (apex–*exo*) bond is low. Subsequent refinements

thus employed a dynamic model incorporating  $p_{10}$  as the potential energy barrier  $V_0$  as described above.

All nine of the independent parameters defining the molecular

**Table 3.** Interatomic Distances ( $r_i$ /pm) and Amplitudes of Vibration ( $u_i$ /pm) for 1-(F<sub>2</sub>B)B<sub>5</sub>H<sub>8</sub><sup>a-c</sup>

		distance	amplitude	
$r_1$	B(2)–B(3)	181.2(6)	7.0(3)	
$r_2$	B(1)–B(2)	170.6(4)	6.6	} (tied to $u_1$ )
$r_3$	B(1)–B(6)	167.6(7)	6.6	
$r_4$	B(6)–F(1)	132.2(3)	4.4(4)	
$r_5$	B(2)–H(2)	119.5(13)	8.4 (tied to $u_6$ )	
$r_6$	B(2)–H(2,3)	138.9(11)	10.9(18)	
$r_7$	B(2)···B(4)	256.3(8)	8.0(f)	
$r_8$	B(2)···B(6)	308.1(4)	10.4(4)	
$r_9$	B(1)···F(1)	263.1(7)	8.0(f)	
$r_{10}$	F(1)···F(2)	223.5(5)	7.0(6)	
$r_{11}$	B(2)···H(3)	278.8(12)	12.4	} (rf)
$r_{12}$	B(2)···H(3,4)	258.1(26)	12.4	
$r_{13}$	B(1)···H(4)	270.3(18)	12.4	
$r_{14}$	B(1)···H(3,4)	247.2(15)	12.4	
$r_{15}$	B(2)···H(4)	375.7(14)	13.1	} (rf)
$r_{16}$	B(6)···H(3,4)	399.5(17)	13.1	
$r_{17}$	B(6)···H(4)	370.9(45)	13.1	
$r_{18}$	B(2)···F(1)	365.8(6)	14.0(13)	
$r_{19}$	B(3)···F(1)	417.3(5)	11.3(6)	
$r_{20}$	B(4)···F(1)	412.5(5)	11.3 (tied to $u_{18}$ )	
$r_{21}$	B(5)···F(1)	360.3(6)	14.0 (tied to $u_{18}$ )	
$r_{22}$	F(1)···H(4)	478.7(41)	18.5	} (rf)
$r_{23}$	F(1)···H(3,4)	509.3(10)	18.5	
$r_{24}$	F(1)···H(3)	486.6(40)	18.5	
$r_{25}$	F(1)···H(2,3)	483.0(14)	18.5	
$r_{26}$	F(1)···H(2)	398.6(52)	18.5	
$r_{27}$	F(1)···H(2,5)	448.7(25)	18.5	
$r_{28}$	F(1)···H(5)	388.9(54)	18.5	
$r_{29}$	F(1)···H(4,5)	477.0(15)	18.5	
$r_{30}$	H(2,3)···H(3,4)	184.6(63)	15.0	} (f)
$r_{31}$	H(2)···H(2,3)	207.1(41)	14.0	
$r_{32}$	H(2,5)···H(3,4)	261.0(89)	18.0	
$r_{33}$	H(2)···H(3)	350.1(16)	18.0	
$r_{34}$	H(2)···H(3,4)	366.4(41)	18.0	
$r_{35}$	H(2)···H(4)	495.1(23)	20.0	

<sup>a</sup> For atom numbering scheme see Figure 3. Figures in parentheses are the estimated standard deviations. <sup>b</sup> An additional 12 B···F and 24 F···H nonbonded distances were also included in the refinements, but are not listed here. <sup>c</sup> Key: rf = refined then fixed; f = fixed.

geometry yielded to simultaneous refinement. The parameters relating to the heavy-atom skeleton ( $p_1$ – $p_4$ ) varied by no more than  $2\sigma$  throughout the course of the refinements. In addition, it was possible to refine most of the amplitudes of vibration at some point in the analysis although only seven could be included in the final refinement.

The geometrical parameters and vibrational amplitudes relating to the positions of the hydrogen atoms were difficult to refine. This is not surprising since the  $r(\text{B–H})$  peaks in the radial-distribution curve are completely obscured by the feature associated with the  $r(\text{B–F})$  interatomic distance. In the final refinement, it was possible to refine both types of  $r(\text{B–H})$  distance, two angles and one vibrational amplitude; strong correlations between these parameters, however, result in relatively large estimated standard deviations for their values. Attempts to refine the vibrational amplitudes  $u(\text{B–H}_i)$  and  $u(\text{B–H}_b)$  independently resulted in both  $u(\text{B–F})$  and  $u(\text{B–H}_i)$  adopting unrealistic values, *i.e.* 3.3(15) and 5.4(32) pm, respectively.

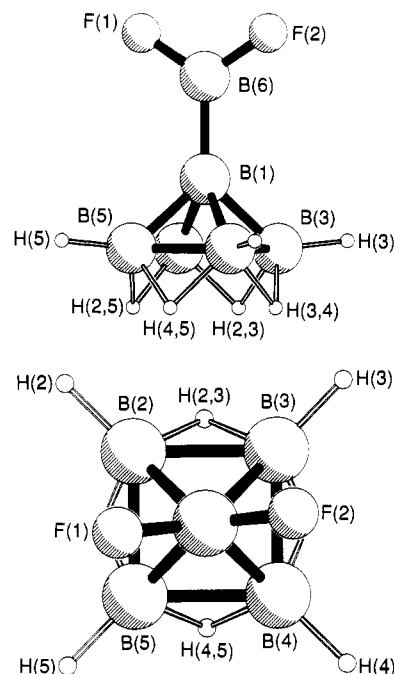
It was not possible to refine the potential energy barrier,  $p_{10}$ , freely. Instead, refinements were undertaken with  $p_{10}$  fixed at increments of *ca.* 0.4 kJ mol<sup>-1</sup> over the range 0.0–4.2 kJ mol<sup>-1</sup>. These refinements were only stable over the range 0.0–2.5 kJ mol<sup>-1</sup> for which the  $R_G$  value increased from *ca.* 0.049 to 0.095. Thus, in the final refinement  $p_{10}$  was fixed at 0.0 kJ mol<sup>-1</sup>.

The success of the final refinement, for which  $R_G = 0.049$  ( $R_D = 0.040$ ), may be assessed on the basis of the difference between

**Table 4.** Least-Squares Correlation Matrix ( $\times 100$ ) for 1-(F<sub>2</sub>B)B<sub>5</sub>H<sub>8</sub><sup>a</sup>

$p_2$	$p_3$	$p_4$	$p_5$	$p_6$	$p_7$	$p_8$	$p_9$	$u_1$	$u_4$	$u_6$	$u_{10}$	$u_{18}$	$k_1$	$k_2$
-53	57				-58		87				74		66	65
	-82						-62	75		53				$p_1$
		62	-52				74	-61						$p_2$
			72											$p_3$
				64	-90	-73	75		52	82		76	54	58
					-60		90		62	80		66		$p_4$
							-65	53	-51	-52	-68	-63		$p_5$
							-61				-71	-67	-71	-82
											65	84	53	86
												54		56
														$p_6$
										56				$p_7$
											52	57		$u_1$
												76	68	70
												56	64	65
													64	65
														86

<sup>a</sup> Only elements with absolute values  $>50$  are shown.  $k$  is a scale factor.

**Figure 3.** Optimum experimental structures of 1-(F<sub>2</sub>B)B<sub>5</sub>H<sub>8</sub>: (a, top) perspective view; (b, bottom) view along the B–B (*exo*-apex) bond.

the experimental and calculated radial-distribution curves (Figure 1). Figure 2 offers a similar comparison between the experimental and calculated molecular-scattering curves whilst salient values of the least-squares correlation matrix are shown in Table 4. The structural details and vibrational amplitudes of the optimum refinement are listed in Table 3; Figure 3a affords a perspective view of the molecule.

The relatively low symmetry of the molecule 1-(F<sub>2</sub>B)B<sub>5</sub>H<sub>8</sub>, allied to the lack of any rigorously based vibrational assignment, ruled out the possibility of applying shrinkage corrections. However, there is no reason to suppose that such corrections would alter the results of the calculations significantly.

**Ab Initio and IGLO Calculations.** The structure of 1-(difluoroboryl)pentaborane(9) was optimized at the HF and MP2 levels of theory; DZ, DZP, and 6-31G\* basis sets were employed to assess the importance of both electron correlation and polarization functions on the quality of such calculations. Total electronic energies were also calculated for wave functions which included higher order correlation corrections than MP2, including Moller–Plesset perturbation theory through third and fourth orders (MP3, MP4), configuration interaction with all single and double electronic excitations from the Hartree–Fock reference wave function (CISD), CISD plus the perturbative estimate for triple

**Table 5.** Theoretical Structural Parameters for 1-(F<sub>2</sub>B)B<sub>5</sub>H<sub>8</sub> (Distances in pm, Angles in deg)

param <sup>a</sup>	φ <sup>b</sup>	level of theory/basis set				
		HF/DZ	MP2/DZ	HF/DZP	MP2/DZP	MP2/6-31G*
p <sub>1</sub> r(B-B)(base-base)	0	186.3/184.4	186.6/184.8	183.1/181.5	180.7/179.2	179.3/178.0
	45	185.3	185.7	182.3	179.9	178.7
p <sub>2</sub> r(B-B)(base-apex)	0	172.1	173.5	171.2	169.8	169.0
	45	172.7/171.6	174.1/172.9	171.7/170.8	170.3/169.3	169.4/168.6
p <sub>3</sub> r(B-B)(apex-exo)	0	165.4	165.9	168.3	166.4	167.1
	45	165.5	166.0	168.4	166.4	167.2
p <sub>4</sub> r(B-F)	0	137.1	140.0	132.1	133.7	134.0
	45	137.0	140.0	132.1	133.7	134.0
p <sub>5</sub> r(B-H)(terminal)	0	117.0	118.4	117.7	117.7	118.6
	45	117.0/117.0	118.5/118.4	117.7/117.7	117.7/117.7	118.7/118.6
p <sub>6</sub> r(B-H)(bridge)	0	136.7/136.8	137.8/137.8	135.3/135.3	134.4/134.3	134.3/134.3
	45	136.2/137.3	137.1/138.5	134.8/135.7	133.8/134.8	133.8/134.7
p <sub>7</sub> FBF	0	112.1	112.5	113.9	114.6	114.9
	45	112.1	112.5	113.9	114.6	114.9
p <sub>8</sub> B-H <sub>t</sub> "rise"	0	11.1	11.0	9.8	9.8	7.2
	45	11.7/10.6	11.7/10.1	10.3/9.3	10.4/9.1	7.6/6.5
p <sub>9</sub> B-H <sub>b</sub> "dip"	0	62.5/62.0	63.0/62.4	63.0/62.4	63.7/63.0	63.6/62.9
	45	62.0	62.3	62.4	63.1	63.5

<sup>a</sup> For definitions of parameters, see the text. <sup>b</sup> φ = angle of rotation of the BF<sub>2</sub> group (φ = 0° defined as having two bridging hydrogens in the BF<sub>2</sub> plane).

**Table 6.** IGLO Results for 1-(F<sub>2</sub>B)B<sub>5</sub>H<sub>8</sub>

molecule	level of theory//geometry	δ( <sup>11</sup> B)/ppm <sup>a</sup>			relative energy/kJ mol <sup>-1</sup>
		B(apical)	B(basal)	B(exo)	
1-(F <sub>2</sub> B)B <sub>5</sub> H <sub>8</sub>	DZ//MP2/6-31G* (0°) <sup>b</sup>	-61.2	-11.1	33.0	0.0
	DZ//MP2/6-31G* (45°) <sup>c</sup>	-61.2	-11.2	33.0	0.1
	DZ//GED	-61.2	-11.4	31.8	14.7
	DZ//GED (H relaxed) <sup>d</sup>	-60.9	-10.0	32.0	3.4
	exptl	-59.3	-13.3	34.5	

<sup>a</sup> Relative to BF<sub>3</sub>OEt<sub>2</sub>. <sup>b</sup> F atoms located above bridging hydrogens. <sup>c</sup> F atoms located above terminal hydrogens. <sup>d</sup> H-atom positions optimized at the MP2/6-31G\* level while holding the heavy-atom skeleton at GED geometry.

excitations [CISD(T)], and quadratic CISD (QCISD); the coupled cluster with double excitations wave function (CCD) and the TZ2P basis set were also employed in this research. Since it was not possible to optimize the structures at such high levels of theory (due to the limitations of computing time), the geometries optimized at MP2/DZ and MP2/DZP levels were employed in these latter energy calculations. Moreover, it has been shown elsewhere that the precision of theoretical geometrical parameters for such systems does not change significantly at computational levels above MP2, even when large basis sets such as TZ2P are used.<sup>22-24</sup> The experimental (GED) and theoretical [MP2(fc)/6-31G\* level] geometries were used to calculate <sup>11</sup>B NMR chemical shifts for 1-(F<sub>2</sub>B)B<sub>5</sub>H<sub>8</sub> using the IGLO method. The calculated values, DZ//MP2/6-31G\* and DZ//GED, are given in Table 6 together with the experimental values.<sup>18,19</sup> In addition, single-point energy calculations at the MP2(fc)/6-31G\* level have been performed for the electron-diffraction structure. The energy relative to the MP2(fc)/6-31G\* fully optimized structure (*i.e.* the minimum on the potential-energy surface) is included in Table 6. Experimental borane and carborane geometries have been assessed previously by means of this "energy criterion".<sup>24a,26</sup>

Two conformations were located on the ground-state potential-energy surface of 1-(F<sub>2</sub>B)B<sub>5</sub>H<sub>8</sub>; these correspond to twist angles of 0° (two H<sub>b</sub> atoms in the BF<sub>2</sub> plane) (conformation 1) and 45° (two H<sub>t</sub> atoms in the BF<sub>2</sub> plane) (conformation 2) of the BF<sub>2</sub> group about the B-B (apex-exo) bond. The calculated geometrical parameters for the two conformations are very similar and are presented in Table 5. Energetically, conformation 1 is calculated consistently to be lower in energy than conformation 2 (see below); conformation 2 corresponds to a transition state for the BF<sub>2</sub> rotation (one imaginary frequency of -8.4 cm<sup>-1</sup> at the RHF/6-31G\* level).

## Discussion

The present measurements on 1-(difluoroboryl)penta borane(9) provide the first structure to be determined for a gaseous compound

of this class, as well as the first structure of a gaseous boron hydride possessing an *exo* σ B-B bond. The analysis of the electron-diffraction pattern endorses the spectroscopic evidence<sup>17-19</sup> that the molecule consists of a square-pyramidal B<sub>5</sub>H<sub>8</sub> cage with a BF<sub>2</sub> group σ bonded to the apical boron atom, B(1). Furthermore, the analysis reveals that the BF<sub>2</sub> moiety is free to rotate about the B-B (apex-exo) bond.

The structural parameters derived by the *ab initio* calculations for 1-(F<sub>2</sub>B)B<sub>5</sub>H<sub>8</sub> (Table 5) are in good qualitative agreement with those refined from the electron-diffraction pattern (Table 2); for example, the predicted B-B bond lengths are in the correct order with *r*(B-B) (base-base) > *r*(B-B)(base-apex) > *r*(B-B)(apex-exo). However, it is clear from Table 5 that good quantitative agreement between the experimental and theoretical results is dependent upon the inclusion of both (i) electron correlation, at the MP2 level or higher, and (ii) polarization functions in the basis set (*e.g.* DZP) in the theoretical calculations. Thus, at the MP2/DZP or MP2/6-31G\* levels, the theoretical parameters offer good support for those derived experimentally.<sup>42</sup> The calculated value of Δ*E* (corresponding to the BF<sub>2</sub> rotational barrier) ranges from 0.84 (MP2/DZ level) to 0.08 kJ mol<sup>-1</sup> (MP2/6-31G\* level) for methods including electron correlation;<sup>43</sup> the value is essentially unaffected by the basis set (generally decreasing slightly with larger basis sets) and the method used to include electron correlation effects (MP2, MP3 *etc.*). The final value of Δ*E* is about 0.25 kJ mol<sup>-1</sup>;<sup>44</sup> in the gas phase at 293 K (*RT* = *ca.* 2.4 kJ mol<sup>-1</sup>) sufficient thermal energy is present to overcome the calculated small barrier and free rotation is the predicted experimental observation.

(42) It should be borne in mind, however, that this procedure involves comparison of two different structure types, namely *r<sub>s</sub>* (from GED) and *r<sub>e</sub>* (from calculations) geometries. See, for example: Hargittai, I.; Hargittai, M.; *Molecular Structures and Energetics*, Vol. II, *Physical Measurements*; VCH Publishers: New York, 1988; Chapter 20, p 417.

(43) A full list of Δ*E* values is given as part of the supplementary material.  
(44) As calculated at our highest attainable level, *i.e.* at the MP2/TZ2P level using the MP2/DZP level optimized geometries.

**Table 7.** Bond Lengths in Boron Hydrides and Related Compounds Containing B–B 2c–2e Bonds<sup>a</sup>

molecule	phase/ technique <sup>b</sup>	r(B–B)(2c–2e)	r(B–F)	ref
2,2'-(B <sub>10</sub> H <sub>13</sub> ) <sub>2</sub>	crystal/XRD	169.2(3)		6
2,6'-(B <sub>10</sub> H <sub>13</sub> ) <sub>2</sub>	crystal/XRD	167.9(3)		6
1,5'-(B <sub>10</sub> H <sub>13</sub> ) <sub>2</sub>	crystal/XRD	169.8(3)		7
1,2'-(B <sub>10</sub> H <sub>13</sub> ) <sub>2</sub>	crystal/XRD	169.6(4)		8
1,1'-(B <sub>5</sub> H <sub>8</sub> ) <sub>2</sub>	crystal/XRD	174(6)		9
2,2'-(1-B <sub>9</sub> H <sub>8</sub> S) <sub>2</sub>	crystal/XRD	167.8(5)		10
I <sup>c</sup>	crystal/XRD	168.1(2)		11
II <sup>c</sup>	crystal/XRD	165.4(8)		12
III <sup>c</sup>	crystal/XRD	170.7(15)		13
1,2'-(B <sub>5</sub> H <sub>8</sub> ) <sub>2</sub>	crystal/XRD	166.0(8)		14
1-(F <sub>2</sub> B)B <sub>5</sub> H <sub>8</sub>	vapor/ED	167.6(7)	132.2(3)	this work
B <sub>2</sub> F <sub>4</sub>	vapor/ED	172.0(4)	131.7(2)	46
B <sub>2</sub> (OMe) <sub>4</sub>	vapor/ED	172.0(6)		21
BF <sub>3</sub>	vapor/ED		131.6(4)	47

<sup>a</sup> Figures in parentheses are the estimated standard deviations. <sup>b</sup> ED = Electron diffraction, XRD = X-ray diffraction. <sup>c</sup> I = 3,8'-(1,2-C<sub>2</sub>B<sub>10</sub>H<sub>11</sub>)(5',6'-C<sub>2</sub>B<sub>8</sub>H<sub>11</sub>); II = 3',2-(2',4'-C<sub>2</sub>B<sub>5</sub>H<sub>6</sub>)(1,8,5,6-[η-C<sub>5</sub>H<sub>5</sub>]<sub>2</sub>-Co<sub>2</sub>C<sub>2</sub>B<sub>5</sub>H<sub>6</sub>); III = 2',4-(B<sub>10</sub>H<sub>13</sub>)(7,7-[(PMe<sub>2</sub>Ph)<sub>2</sub>]-7-PtB<sub>10</sub>H<sub>11</sub>).

Further evidence for the accuracy of the electron-diffraction structure of 1-(F<sub>2</sub>B)B<sub>5</sub>H<sub>8</sub> comes from the calculation of the δ(<sup>11</sup>B) values and the relative energy (Table 6). The IGLO <sup>11</sup>B chemical shifts differ by no more than 2.7 ppm from the experimental values, and the experimental geometry is calculated to be only 14.7 kJ mol<sup>-1</sup> higher in energy than the fully optimized theoretical structure. Such an "excess energy" is found to be in the normal range for similarly large boranes and carboranes.<sup>24a,26</sup> A partial optimization of the electron-diffraction structure at the MP2(fc)/6-31G\* level was also undertaken in which the heavy-atom skeleton remained fixed but the locations of the hydrogen atoms were permitted to vary.<sup>45</sup> This so-called "hydrogen-relaxed" GED geometry of 1-(F<sub>2</sub>B)B<sub>5</sub>H<sub>8</sub> optimized to a structure with a calculated energy of only 3.4 kJ mol<sup>-1</sup> greater than that for the fully optimized theoretical structure. Thus, the "excess energy" calculated for the new GED structure is attributable almost completely to the positions of the hydrogen atoms.

Table 7 summarizes the structural details derived to date for boron hydride compounds with *exo* 2c–2e B–B bonds, together with corresponding parameters of some diboron and other boron fluoride molecules. Although care must be exercised in comparing results derived from different structural techniques, it would appear that the *exo* B–B bond length calculated for 1-(F<sub>2</sub>B)B<sub>5</sub>H<sub>8</sub> is typical of the values found for most of the other boron hydride systems possessing *exo* B–B bonds. Comparison with the apparently large value ascribed to the corresponding distance in 1,1'-(B<sub>5</sub>H<sub>8</sub>)<sub>2</sub><sup>9</sup> is meaningless in view of the very large estimated standard deviation for the *conjuncto* boron hydride. The length of the σ B–B bond in these types of compound is governed by several factors, e.g. the charge density at the boron atoms and

the size of the units bonded together by the σ B–B bond, their rigidity, and nonbonded interactions. It is our intention to explore the relative contributions made by these factors in a study of related compounds. The B–B bonds in the diboron compounds are longer than the 2c–2e bond of the boron hydrides. Larger nonbonded interactions across the B–B bond in the diboron systems are probably the dominating feature here.

At 132.2 pm, the B–F bond length in 1-(F<sub>2</sub>B)B<sub>5</sub>H<sub>8</sub> is only slightly longer than that observed for B<sub>2</sub>F<sub>4</sub><sup>46</sup> and BF<sub>3</sub>.<sup>47</sup> It would appear that a significant amount of π character contributes to the B–F bonding in all of the molecules.

The geometry of the B<sub>5</sub>H<sub>8</sub> cage in 1-(difluoroboryl)pentaborane(9) is similar in most respects to that of pentaborane(9) itself.<sup>15</sup> Bearing in mind the large estimated errors associated with their positions, we note that the bridging hydrogens subtend the same angle with the basal plane although the B–H<sub>t</sub> "rise angle" appears to be *ca.* 12(8)° lower in the case of 1-(F<sub>2</sub>B)B<sub>5</sub>H<sub>8</sub>, presumably through an increase in nonbonding interactions relative to B<sub>5</sub>H<sub>9</sub>. It is interesting to note that the B–B (base-apex) bond lengths in 1-(F<sub>2</sub>B)B<sub>5</sub>H<sub>8</sub> are attenuated by 1.2(6) pm compared with those in B<sub>5</sub>H<sub>9</sub>. A similar observation has also been made for other σ B–B bonded boron hydrides for which structural information is available; for example, the intracage B–B(1) and B–B(2') bond lengths in 1,2'-(B<sub>10</sub>H<sub>13</sub>)<sub>2</sub> are found to be 1–3 pm longer than the corresponding distances in B<sub>10</sub>H<sub>14</sub>.<sup>8</sup> This may be indicative of increased electron demand for σ B–B *versus* *exo*-terminal B–H bond formation.

**Acknowledgment.** We thank the SERC for support of the Edinburgh Electron-Diffraction Service, including provision of microdensitometer facilities at the Daresbury laboratory and research fellowships for P.T.B. and H.E.R. We gratefully acknowledge Dr. P. L. Timms (University of Bristol) and Dr. P. Grebenik (Oxford Brookes University), for the supply of essential starting materials and Dr. A. J. Downs (University of Oxford) for the provision of laboratory facilities during a short visit to prepare the sample. We are indebted to Mr. N. K. Mooljee of the Edinburgh University Computing Service for technical assistance during the course of this work. The work in Erlangen was supported by the Deutsche Forschungsgemeinschaft and the Fonds der Chemischen Industrie. We thank Prof. W. Kutzelnigg and Dr. M. Schindler for the Convex version of their IGLO program. I.L.A. acknowledges support of the SERC via Grant GR/H/30373 and access to the Convex C3840 at ULCC.

**Supplementary Material Available:** Tables of (i) atomic coordinates for the final experimental structure and (ii) the theoretical energy differences for the two conformations (2 pages). Ordering information is given on any current masthead page.

(45) See also: McKee, M. L. *J. Phys. Chem.* **1990**, *94*, 435.

(46) Danielson, D. D.; Patton, J. V.; Hedberg, K. *J. Am. Chem. Soc.* **1977**, *99*, 6484.

(47) Konaka, S.; Murata, Y.; Kuchitsu, K.; Morino, Y. *Bull. Chem. Soc., Jpn.* **1966**, *39*, 1134.